Hydrol. Earth Syst. Sci. Discuss., 11, 10043–10084, 2014
www.hydrol-earth-syst-sci-discuss.net/11/10043/2014/
doi:10.5194/hessd-11-10043-2014

Hydrology and Earth System Sciences
Open Access
Discussions

Derivation of a new continuous adjustment function for correcting wind-induced loss of solid precipitation: results of a Norwegian field study

M. A. Wolff[1], K. Isaksen[1], A. Petersen-Øverleir[2], K. Ødemark[1], T. Reitan[3], and R. Brækkan[1]

[1]Norwegian Meteorological Institute, Oslo, Norway
[2]Statkraft, Oslo, Norway
[3]Norwegian Water Resources and Energy Directorate, Oslo, Norway

Received: 24 June 2014 – Accepted: 6 August 2014 – Published: 1 September 2014

Correspondence to: M. A. Wolff (mareilew@met.no)

Published by Copernicus Publications on behalf of the European Geosciences Union.

Abstract

Precipitation measurements exhibit large cold-season biases due to under-catch in windy conditions. These uncertainties affect water balance calculations, snowpack monitoring and calibrations of remote sensing algorithms and land surface models. More accurate data would improve the ability to predict future changes in water resources and mountain hazards in snow-dominated regions.

In 2010, an extensive test-site for precipitation measurements was established at a mountain plateau in Southern Norway. Precipitation data of automatic gauges were compared with a precipitation gauge in a Double Fence Intercomparison Reference (DFIR) wind shield construction which served as the reference. Additionally, a large number of sensors were monitoring supportive meteorological parameters.

In this paper, data from three winters were used to study and determine the wind-induced under-catch of solid precipitation. Qualitative analyses and Bayesian statistics were used to evaluate and objectively choose the model that is describing the data best. A continuous adjustment function and its uncertainty were derived for measurements of all types of winter precipitation (from rain to dry snow). A regression analysis did not reveal any significant misspecifications for the adjustment function, but showed that the chosen model uncertainty is slightly insufficient and can be further optimized. The adjustment function is operationally usable based only on data available at standard automatic weather stations.

Our results show a non-linear relationship between under-catch and wind speed during winter precipitation events and there is a clear temperature dependency, mainly reflecting the precipitation type. The results allowed for the first time to derive an adjustment function with a data-tested validity beyond 7 m s^{-1} and proved a stabilisation of the wind-induced precipitation loss for higher wind speeds.

HESSD
11, 10043–10084, 2014

1 Introduction

Climate predictions suggest also major changes in the hydrological cycle, beside the rising global temperature. Water and the availability to water are indispensable to life. More than one-sixth of Earth's population gets most of their water supply from glaciers and seasonal snow packs and many of these are in jeopardy (Barnett, 2005). Precipitation observations are important to describe the hydrological cycle quantitatively. Their accuracy needs to be improved further to allow for a better evaluation and verification of numerical weather forecast, hydrological, and climate models. Thus enhancing these models' capabilities to predict short and long term changes as well as variability of the world's water budget with greater confidence (Seneviratne et al., 2012).

It has been known for a long time that especially measuring precipitation in the form of snow is difficult. The fact that wind induces a bias on solid precipitation measurements is well established. E.g. Brown and Peck (1962) addressed the challenges of precipitation measurements related to exposure in 1962. This systematic under-catch can be reduced by shielding the gauge, and various types of windshield configurations have been developed for this purpose (e.g Alter, Tretyjakov). Nevertheless, wind bias still remains evident in snow measurements, and requires an adjustment. In the 1980s, methods for correcting systematic errors in precipitation measurements for operational use were suggested, described in Sevruk (1982).

The most recent comprehensive study was the study organized by the WMO Solid Precipitation Intercomparison Committee between 1987 and 1993 (Goodison et al., 1998). An outcome of the study was the recommendation of the Double Fence Intercomparison Reference, DFIR, as the reference for which snow measurements should be compared to. The study assessed and derived adjustment functions for measurements configurations for solid precipitation used at that time, which to a large extent were manual observations.

Førland et al. (1996) developed and described a more operational method for correcting precipitation measurements in Nordic countries based on the findings of the

HESSD
11, 10043–10084, 2014

Jokioinen test site in Finland as described in Goodison et al. (1998). These methods or variations of it (i.e. Hansen-Bauer et al., 1996) are in wide use by Norway's hydropower companies whose budget calculations highly depend on accurate precipitation measurements.

Another large scale application of the adjustment functions from Goodison et al. (1998) for daily observations of Nordic precipitation stations (north of 45° N) across national boundaries were performed by Yang et al. (2005). The resulting adjustments could be shown to have a tremendous effect on the existing and future precipitation data set because of their order of magnitude that additionally varies dependent on the local climate.

Førland and Hansen-Bauer (2000) analysed and adjusted precipitation measurements at Svalbard. Temperatures are significantly rising in the Arctic and already today falls a larger fraction of the annual precipitation as rain than earlier. This results in a fictitious increase of precipitation amount, as rain is less affected by the wind induced bias than snow. Førland and Hansen-Bauer (2000) could show that this non-real increase of precipitation amount is in the magnitude of the expected real increase of precipitation amount due to climate change.

Rasmussen et al. (2012) present recent efforts to understand the relative accuracies of different instrumentation, gauges, and windshield configurations to measure snowfall that have been developed since the WMO Intercomparison Test of Solid Precipitation (1989–1993), at the National Center for Atmospheric Research (NCAR) Marshall Field Site.

In recent years, an increasing number of stations were automated. However, information regarding measurement uncertainty for automatic measurements is lacking. While there are several studies on measurements of solid precipitation, only a few focuses on the accuracy of automatic precipitation measurements (Rasmussen et al., 2012). This problem is also given focus in the IPCC AR5 (Bindoff et al., 2013) which states that observational uncertainties, in addition to challenges in precipitation modelling, limit confidence in assessment of climatic changes in precipitation.

HESSD
11, 10043–10084, 2014

From 2008 to 2009, performance of a large number of precipitation gauges and windshield configurations were evaluated towards a DFIR at Environment Canada's CARE and Bratt's Lake sites, Smith and Yang (2010) and Rasmusssen et al. (2012). A survey was conducted by Nitu and Wong (2010) to develop a summary of current methods and instruments for measuring solid precipitation. They stated that the variation in gauges and windshield configurations is much larger for automatic stations than for manual stations. The results indicated further that a review of the current state-of-the-art methodologies is required to increase the precipitation measurement accuracy. Following that, The Commission for Instruments and Methods of Observations (CIMO) within WMO took on a leadership role for evaluating gauges for solid precipitation measurements in cold and Alpine climates within the WMO-CIMO Solid Precipitaion Intercomparison Experiment (WMO-SPICE). Here, several countries participate in the development of a new set of adjustment functions, with host-sites comparing precipitation data of different automatic gauges with data of a reference gauge with the recommended DFIR-construction.

This paper presents the results from the Norwegian test site located on a mountain plateau in Southern Norway. The site was established in 2010, as an initiative from Norway's hydropower companies in the need of accurate snow measurements for predicting water resources. Besides its original purpose, the site became additionally a host-site for WMO SPICE in 2013 and will continue operating as a long-term reference station for monitoring the changes in precipitation amount in Norway. Furthermore, the station is also part of a newly established national network for improved avalanche forecasting.

The objective of this study is to determine the wind-induced under-catch of solid precipitation and develop a continuous adjustment function for measurements of all types of winter precipitation (from rain to dry snow), which can be used for operational measurements based on data available at standard automatic weather stations. Qualitative analyses and Bayesian statistics are used to evaluate and objectively choose the model describing the data best.

HESSD
11, 10043–10084, 2014

The chosen locality has proven to be ideal for this purpose. The site experiences a lot of snow, often accompanied by high winds – which gives many interesting events for studying the wind induced influence on solid precipitation. The high winds have contributed to making a unique dataset when compared to other test-sites, where such high winds are not as common.

The measurement site is described in chapter two, which presents an overview of the settings and climatology of the area. Chapter three describes the data preparation done in advance of the main analysis, as well as the qualitative and quantitative analyses methods used. Results are presented in chapter four, followed by a discussion and conclusions in chapter five and six, respectively.

2 Measurement site

2.1 Setting

Haukeliseter test-site is situated on a mountain plateau in Southern Norway (59.82° N and 7.21° E at 991 m a.s.l.), see Fig. 1. All instruments are placed on a 5000 m^2 flattened area, surrounded by topographic variations up to 20 m in immediate vicinity and then slowly increasing to the surrounding mountain tops which are between 100 and 500 m higher.

The area is situated between two lakes and the closest top (distance 1 km) has an altitude of 1162 m a.s.l. in North-east direction. The tops in eastward direction reach ca. 1250 m a.s.l. in a distance of 2 km. The terrain is more open towards South and West with 4 km and 3 km to the closest tops, respectively.

Precipitation sensors are mounted side by side perpendicular to the prevailing wind directions from easterly and westerly directions in order to minimize mutual disturbances. The reference configuration at Haukeliseter consists of an automatic precipitation gauge (Geonor T200-BM, 1000 mm, 3 transducers; Geonor AS, Norway) and an Alter wind shield, both centred in an octagonal double fence (DF) construction which

HESSD
11, 10043–10084, 2014

effectively minimizes wind influence on the precipitation measurements. The DF is similar to the Double Fence Intercomparison Reference (DFIR) of the first WMO intercomparison (Goodison et al., 1998) where it was used with a Tretyakov manual gauge. The combination of DF and automated gauge at Haukeliseter also fulfils the specifications for the official DFAR (Double Fence Automated Reference) of the ongoing WMO-SPICE (WMO/CIMO, 2012) study where Haukeliseter participates as one of currently 20 host-sites worldwide.

Further information about the test-site, amongst others an evaluation of the homogeneity and a list of instruments, can be found in Wolff et al. (2010, 2013).

2.2 Climate

Haukeliseter testsite was chosen because of its significant amount of snow events often paired with high wind speeds during the 6 to 7 months long winters. Solid precipitation is very usual between October and May and can also occur during the summer months. The estimated mean annual air temperature (MAAT, 1961–1990) for the site is 0.6 °C. Mean monthly temperatures are below 0 °C for the period November to April, with an estimated mean air temperature (1961–1990) of −5.4 °C. The estimated, uncorrected annual precipitation (1961–1990) is approximately 800 mm whereof more than 50 % is solid precipitation. In a normal winter, the average snow depth reaches approximately 1.5–2.0 m.

Further, 10 years of winter observations from a nearby manual station operating between 1984 and 1995 reported a sufficient amount of snow events with maximum wind speed above 15 m s^{-1}. These observations also reported a frequent occurrence of blowing and drifting snow, a significant amount of these below eye-height. Precipitation gauges at Haukeliseter were therefore mounted at relatively high 4.5 m to minimize the influence of blowing and drifting snow on the measurements.

Data for this study were collected over the course of three winters, starting early 2011 until May 2013. Figure 2 shows the monthly precipitation and mean temperature anomaly in respect to the normal period 1961–1990 for all measurement months,

HESSD
11, 10043–10084, 2014

based on data from the official nearby meteorological station Vågsli (821 m a.s.l., located 10 km eastwards). The months that are not shown here were used for maintenance and upgrading works at the test site.

All three months of the first period in 2011 are characterized by a higher precipitation amount than normal. Whereas February 2011 was relatively cold, were March and April 2011 rather warm. April 2011, with a mean temperature of 4.8 °C above normal monthly mean temperature, was registered as the warmest April since 1900 in large areas of Southern Norway.

The second winter (November 2011–April 2012) was continuously mild (with exception of April 2012) and a higher precipitation amount than usual was registered (with exception of March 2012). In December 2011, more than double of the normal monthly precipitation amount was observed. March 2012 was the warmest month ever recorded in Western and Eastern Norway. The mean temperature at Vågsli was 6.2 °C above normal monthly temperature.

The third winter was characterized by low temperatures. Whereas during February and March 2013 very little precipitation was registered, April and May 2013 were characterized by very high precipitation amounts.

3 Data and methods

Measurements from all precipitation instruments and meteorological auxiliary measurements are monitored every minute from two combined data loggers (SM5049 by Scanmatic AS, Norway). Data are transferred hourly to the Norwegian Meteorological Institute (MET Norway) and stored in the official Climate data base, assuring long term storage and availability for data analysis.

HESSD
11, 10043–10084, 2014

3.1 Data preparation

3.1.1 Precipitation events

An algorithm was developed to guarantee an objective and comparable method for identifying precipitation periods with significant and for the most part continuous accumulation. The algorithm was applied on the complete dataset containing 10 min running averages of the measurements by the DF-Geonor and a precipitation detector (Yes/No).

The following thresholds were used to check for (a) continuity and (b) significance of the precipitation periods:

a. 8 of 10 min have to have registered precipitation (from precipitation detector).

b. Accumulation has to be more than 0.1 mm per 10 min or, in case of event duration longer than 100 min, more than 1 mm for the entire event period.

The resulting precipitation periods were of various lengths and were divided into 10 and 60 min events respectively. The complete event data set contained the identified periods, accumulation measured in all precipitation gauges, mean and standard deviation of temperature, wind speed, wind direction and humidity, net precipitation time in minutes and typical weather codes as measured from the present weather sensor.

The introduction of thresholds implies that events interrupted by breaks or characterized by a very low accumulation rate are ignored. Furthermore, an event might start and/or end with a lower rate and might therefore not being registered over its full length. The described method, however, guaranteed that only unambiguous events were used in the following analysis and thus determining dependencies with higher accuracy.

The qualitative analysis was performed on both 10 and 60 min events. Only the 60 min events are shown, as no significant differences occurred. The quantitative analysis was performed on 60 min events only.

HESSD
11, 10043–10084, 2014

3.1.2 Wind measurements in 10 m height and gauge height

Wind measurements at the test site are performed by different sensors, ultra sonic and mechanical (propel), mounted at 10 m (standard height) and gauge height. Before 2013, gauge height wind measurements were solely performed from sensors directly installed to the precipitation gauges. Comparisons with a gauge-height wind sensor on a separate mast (installed in 2013) confirmed the expected impact of the close-by precipitation gauge and wind shield on the wind measurements of the first sensors. Wind directions between 0 and 240° were affected.

For the further analysis with gauge-height wind data, only precipitation events with wind directions from non-affected sectors were considered. Analysis was also performed with wind data from the 10 m sensor, mounted on top of a mast, thus featuring an undisturbed data series. For these data no filtering was necessary and the analysis was performed with the undisturbed data set. These two data sets are hereafter referred to as "gauge-height-wind data set" and "10 m wind data set".

3.2 Data filtering

Catch ratios between standard Geonor configurations and the DF-Geonor for all identified events were calculated. Figure 3 shows the results for the southern Geonor precipitation gauge X2 (see layout in Fig. 1), as this sensor provided the most stable dataset. The large amount of scatter visible in panel a (all events) including some very clear outliers made it necessary to evaluate the influence of various parameters in more detail.

A few negative catch ratios are visible in panel a, which are mainly due to only small accumulation inside the DF-Geonor and no significant accumulation in the X2-Geonor. For these cases the noise of the transducers dominates the X2-signals. They subsequently vary around zero, thus resulting in negative catch ratios. For panel b an additional threshold was introduced, accepting only events for which the X2-Geonor collected more than 0.1 mm, thus removing the unrealistic very small or negative catch

HESSD
11, 10043–10084, 2014

ratios. About 5 % of the recorded events inside the DF at Haukeliseter are showing no significant accumulation in the gauges outside.

As the installations are optimized for minimized influence under prevailing wind directions (installation along a line, see site layout in Fig. 1), are shadowing effects likely for other wind directions. Geonor X2 will be mostly affected by shadowing for wind directions between 355 and 55°. Panel c shows all events where these wind directions are removed using data from the wind sensor at 10 m height. The resulting data points show little less scatter for lower wind speeds. The effect is more visible when considering only snow events. Panels g and h show the filtered data for temperature < 0 °C and temperature < −2 °C, respectively.

Variations of both, temperature and wind speed during an event were evaluated. Events with a standard deviation smaller than 0.2 °C during the event period are shown in panel e, further thresholds were tested (not shown). It seemed most natural to weigh wind speed variations with the mean wind speed. The maximum ratio between the standard deviation of wind speed and the mean wind speed was set to 0.2 for the events shown in panel f. These filter methods for temperature and wind speed variations, did not improve the catch ratio dataset from Haukeliseter. Removed data points are evenly spread and no significant noise reduction was achieved. Therefore, no thresholds for limiting temperature and wind speed variations were used for the further analysis.

3.3 Qualitative analysis

In a further step, the data set was analysed qualitatively in order to get a more detailed understanding of how the catch ratio is influenced by various parameters. For this purpose, the dataset was divided into classes for temperature, wind, precipitation type and intensity.

HESSD
11, 10043–10084, 2014

3.3.1 Temperature

Fig. 4 shows the catch ratio for different temperature classes in 1 K steps. For temperatures above 2 °C, where precipitation is mainly falling as rain, the catch ratio is not influenced significantly by the wind. For temperatures below −2 °C, where precipitation is mainly falling as snow, the catch ratio curve has a characteristic shape, indicating a clear dependence on the wind speed. This relationship does not change significantly for further decreasing temperatures.

For temperatures between 2 and −2 °C, where snow, rain and mixed precipitation can appear, an increased scatter is visible in the data, obviously depending on the precipitation type for each individual event. The four temperature classes in this region, however, are still suggesting a continuous change from higher to lower temperatures. That is consistent with a larger possibility for rain or very wet snow for temperatures close to +2 °C and a larger possibility for snow for temperatures close to −2 °C.

3.3.2 Wind

Concentrating only on snow data, thus reducing the scatter due to varying precipitation types, data was collected into wind speed classes. The average catch ratios for stepwise increasing wind speed classes are shown in Fig. 5 and suggest a non-linear dependence on the wind speed. After a steep slope with increasing wind, the catch ratio seems to stabilize around 20 % for wind speeds higher than 7–8 m s^{-1}. No obvious temperature dependence for these lower temperature classes can be seen.

3.3.3 Precipitation type

One forward scatter type instrument and two disdrometers were partly available for the determination of the precipitation type. Figure 6 shows a histogram displaying the number of events with different precipitation types and temperatures as observed from the Vaisala PWD 21 (forward scatter type instrument, Vaisala Oyj, Finland).

HESSD
11, 10043–10084, 2014

The data are reporting snow events between +5 and −17 °C, with a maximum at −1 °C and a second smaller maximum around −15 °C. Rain is reported at temperatures down to −1 °C and mixed precipitation was observed between −1 and 5 °C.

A closer look at the snow events (as determined by the Vaisala PWD, not shown) revealed that a robust and consistent result was not possible without further information. The temperature data set and the data from the disdrometer type instruments (where available) suggested that a significant amount of the detected snow events were rather rain events.

This study did not use the precipitation type information further for the development of the adjustment equation. Beside the need for improving the reliability, are these data presently not available for the majority of the Norwegian standard weather stations

Further analysis of these data and an optimized use of the instruments and their capacities in order to determine the precipitation type will be performed in the framework of WMO-SPICE.

3.3.4 Precipitation intensity

Based on the observed precipitation intensity of the precipitation events a simple analysis was performed to detect any dependency of the catch ratio on the precipitation intensity. No significant influence of the precipitation intensity could be identified in the presented winter precipitation data set.

3.4 Quantitative analysis

The qualitative analysis indicated a clear temperature dependence of the catch ratio and a non-linear relationship with wind speed. Precipitation events which were clearly identified as rain or dry snow showed two very different catch ratio relationships. It was, however, desirable to develop only one transfer equation considering a continuous transfer from dry snow over mixed precipitation to rain based on data available at standard weather stations: precipitation, wind and temperature.

HESSD
11, 10043–10084, 2014

3.4.1 Existing adjustment functions used in Norway

The literature on mechanistic relationship between true and measured solid precipitation, given other determinants, is quite scant. Most studies propose relationships that are, to a large extent, empirical, and probably not generic. The most used set of transfer functions for Geonor gauges in cold climate used in the Nordic countries are presented in Førland et al. (1996). The solid form formula has the form:

$$p_T = p_M g_1(V,T) = p_M e^{(b_0 + b_1 V + b_2 T + b_3 V T)} \quad (1)$$

where p_T is true precipitation, p_M is measured precipitation, T is air temperature, V is wind speed at gauge height and (b_0, b_1, b_2, b_3) are parameters. In the same report a related relationship for liquid precipitation is presented:

$$p_T = p_M g_2(V,T) = p_M e^{[c_0 + c_1 V + c_2 \log(I) + b_3 V \log(I)]}, \quad (2)$$

where I is intensity, which in most practical applications must be approximated with p_M. If the exponents in Eqs. (1) and (2) become negative, it is set to zero (no adjustment).

The criteria for using the different transfer functions for the different precipitation types are dependent on temperature:

$$p_T = \begin{cases} p_M g_1(V,T) & T \le 0.0\,^\circ\mathrm{C} \quad \text{snow} \\ p_M g_1(V,T) + p_M g_2(V,T) & 0.0 < T \le 2.0\,^\circ\mathrm{C} \quad \text{mixed precipitation} \\ p_M g_2(V,T) & T > 2.0\,^\circ\mathrm{C} \quad \text{rain} \end{cases} \quad (3)$$

One immediate criticism of the aforementioned framework of formulas is the lack of continuity between segments when the temperature varies over the limits during an event. Furthermore, the limit criteria in Eq. (3) also exclude the possibility of solid precipitation when the temperature is above 2 °C. Similarly, it is assumed that liquid or mixed precipitation does not occur in cases where the temperature is below 0 °C.

HESSD
11, 10043–10084, 2014

Equation (2) includes intensity for mixed and liquid precipitation. Especially during summer, a wide spectrum of very different precipitation events may occur, also including large differences of typical drop sizes. That let expect that intensity as an indirect measure of drop size may also affect the catch ratio. Unfortunately, the true intensity cannot be measured directly since measured precipitation is intrinsically affected by wind induced loss. The approximation becomes especially inaccurate when the temperature is in the area where mixed precipitation occurs.

The equations have a validity limited to events with wind speeds lower than $7\,\mathrm{m\,s^{-1}}$ and temperatures higher than $-12\,^{\circ}\mathrm{C}$, as no data beyond this range were available at the time of derivation.

3.4.2 Preparative assumptions

Based on: (i) a study of the characteristics of similar data in other studies (i.e. Rasmussen et al., 2012), (ii) contemplating existing adjustment functions (i.e. Goodison et al., 1998), (iii) results from theoretical fluid mechanical studies on rain gauges in wind fields (i.e. Thériault et al., 2012; Nešpor and Sevruk, 1999), (iv) what data is commonly available at a typical meteorological station; and (v) an analysis of the collected data at Haukeliseter during winter, the following attributes for an adjustment function, for a given temperature are proposed:

1. The ratio between true and observed precipitation is a function of only wind speed.
2. The ratio is monotonically decreasing from unity when $V = 0$ to a limit greater or equal to zero when the wind speed V approaches infinity.
3. The ratio decreases exponentially as a function of wind speed.
4. The rate of change of ratio varies significantly as a function of wind speed, and can take the value of zero in parts of the domain.

HESSD
11, 10043–10084, 2014

Based on these criteria, a natural choice is a version of Eq. (1) which is non-linear in logarithmic space for a given temperature:

$$R|T = \frac{p_M}{p_T} = (1-\tau)e^{-(\frac{V}{\theta})^{\beta}} + \tau \quad (4)$$

where $\boldsymbol{\varphi} = (\tau, \beta, \theta)$ is the vector of parameters dictating the shape of the relationship.

Equation (4) can be characterised as a bell function, and is generally able to emulate monotonically decreasing functions in the first quadrant. The derivation dR/dV approaches zero in the two endpoints for $\beta > 1$ (which is assumed to be the case), and can have this property in a large part of the actual domain, if necessary.

Furthermore, it is assumed that the characteristics of Eq. (4) vary with temperature. Generally, this can be achieved by formulating the three parameters as functions of temperature, i.e.:

$$R = f(V,T) = [1-\tau(T)]e^{-\left[\frac{V}{\theta(T)}\right]^{\beta(T)}} + \tau(T) \quad (5)$$

The next intuitive question would be: what are the plausible characteristics of the parameter functions $\varphi(T)$? An immediate assumption is that the value of the parameters goes from one limit to another when the temperature increases/decreases. Next, it is proposed that the change of value is at its greatest when the temperature passes through the transition area from dry snow to mixed precipitation. This presumption implies that the parameter functions reach stable values as the temperature moves away from the phase-shift area. These assumptions fit with the pre-analysis of the collected data. They also correspond with Eq. (1).

Furthermore, a continuous transition from dry snow precipitation to mixed precipitation, and perhaps also towards liquid precipitation is wanted. In this context, the question of whether intensity could be a significant determinant arises. As this study focusses on winter precipitation only, intensity is assumed to be negligible.

HESSD
11, 10043–10084, 2014

The aforementioned assumptions imply that the parameter functions are well described by sigmoid functions:

$$\varphi(T) = \varphi_1 + (\varphi_2 - \varphi_1)\frac{e^{(T-T_\varphi)/s_\varphi}}{1 + e^{(T-T_\varphi)/s_\varphi}} \tag{6a}$$

This type of function has the property of approaching the left limit φ_1 when $T \ll T_\varphi$, and the right limit φ_2 when $T \gg T_\varphi$. The parameter T_φ decides the location of the transition between the two limits, while s_φ dictates the fuzziness of the transition. A small s_φ indicates a rapid change, whereas a large value gives an approximately linear transition. For generality, the number of limits can be increased by using higher order functions. This study applies only two and three level functions. The three level expressions were constructed using two non-normalised normal distribution functions having the same mode to ensure a continuous translation. Hence this function had a parameter formulating the middle level and two scale parameters determining the fuzziness in the transition between the levels. Mathematically, that can be expressed by:

$$\varphi(T) = I(T < T_\varphi)\left[\varphi_1 + (\varphi_2 - \varphi_1)e^{-\frac{(T-T_\varphi)^2}{2\cdot s_{\varphi,1}}}\right] + I(T \geq T_\varphi)\left[\varphi_3 + (\varphi_2 - \varphi_3)e^{-\frac{(T-T_\varphi)^2}{2\cdot s_{\varphi,2}}}\right] \tag{6b}$$

The letter I symbolises an indicator function that becomes zero if the inequality inside the parenthesis is false and one otherwise. Furthermore, the left and right hand limits are given by φ_1 and φ_3, while the mode of the middle segment is given by φ_2.

3.4.3 Statistical inference method

In general, multi-level parameter functions opens up the possibility for a lot of plausible model forms. A priori, no combination can be ruled out. A statistical model selection method is thus warranted. The Bayesian machinery is attractive in this respect, since it allows the use of prior knowledge. Given a dataset D from the Haukeliseter test site that

HESSD
11, 10043–10084, 2014

contains $i \in (1, \ldots, n)$ concurrent observations of ratio, wind speed and temperature, a general regression is given by:

$$R_i = [1 - \tau(T_i)]e^{-\left[\frac{V}{\theta(T_i)}\right]^{\beta(T_i)}} + \tau(T_i) + \sigma(T_i)\varepsilon_i, \quad (7)$$

where ε_i is normally distributed noise with zero expectancy and unity variance and σ is an unknown parameter governing the variance of the measurement error. Considering up to three-level sigmoid functions on each of the four parameters in Eq. (7), yields 81 possible sub-models. The simplest is of course the one where all parameter are fixed, and the most complex one is where all four parameters are formulated as three-level sigmoid functions. The latter involves 24 unknown parameters that have to be estimated.

Bayesian Model Likelihood (BML) was used as a model selection tool in this study. Mathematically, it is given by:

$$\mathrm{BML}_M \equiv f(D|M) = \int f(D|\underline{\Omega}_M, M) f(\underline{\Omega}_M|M) d\underline{\Omega}_M \quad (8)$$

where D represents the dataset, M denotes one of the 81 possible models, i.e. $M \in (1, \ldots, 81)$, and $\underline{\Omega}_M$ symbols the set of parameters associated with model M. The quantity $f(\underline{\Omega}_M|M)$ is the prior distribution of parameter set, summarizing our knowledge of what constitutes reasonable parameter values prior to the data. The BMLs give the probability of the data for each proposed model. Those can be used for producing model probabilities or be compared directly between models. We opted for the latter approach. The integral in Eq. (8) cannot be evaluated analytically. Therefore numerical methods have to be used. This study applied an importance-sampling technique described in Reitan and Petersen-Øverleir (2008) where it was used to select segmentation models in hydraulic rating curve analysis.

For each model, Bayesian methods were used for evaluating the model parameters. The posterior distributions of the parameters express the knowledge concerning the

HESSD
11, 10043–10084, 2014

parameters after analysing the data. They are numerically calculated from the prior distribution and the likelihood, Eq. (7), using a MCMC (Markov Chain Monte Carlo) scheme. The algorithm was based on a relatively general random walk Metropolis algorithm along with an adaptive burn-in routine and a parallel tempering approach, Chib and Greenberg (2001). More details on Bayesian data analysis and methods are given in textbooks such as Gelman et al. (2013).

The overall distribution for the parameter set was constructed by assuming prior independence for each parameter logit(τ), log(θ), log(β) and log(σ). The logit function logit(τ) = log($\tau/(1-\tau)$) was used in order to restrict τ to be a number between 0 and 1. The aforementioned re-parameterisation assumes that all parameters are positive a priori. All parameters take values from $-\infty$ to $+\infty$ in logarithmic space. A mathematical tractable and also plausible assumption of normal prior distributions could then be made, presupposing that the parameters were statistically independent a priori. All priors were given mean 0 and standard deviation 10. This constitutes a set of very wide priors that allows for both very small and very large parameter values on the original scale. The reason for this was to avoid the effect of prior information in the subsequent model choice procedure.

The three favoured models from this initial run were chosen and fine-tuned in a second step: information from other datasets (i.e. Rasmussen et al., 2012 and Thériault et al., 2012) and parameters of associated estimated adjustment functions (of different form) were used to derive more informative priors. Still, the priors were constructed relatively wide to avoid misspecifications. Normal distributions were used for the transformed parameters with means and the following 95 % credibility intervals; $\theta \in (1, 20)$, $\beta \in (0.25, 5)$, $\sigma \in (0.001, 1)$, $\tau \in (0.001, 0.999)$. For the two-level temperature dependence, more specific priors $\tau_1 \in (0.001, 0.5)$ and $\tau_2 \in (0.5, 0.999)$ were defined, assuming an asymptotic limit for R as a function of velocity to be larger for high temperatures than for low.

HESSD
11, 10043–10084, 2014

4 Results

The BML analysis quite clearly favoured a model with constant θ and β parameters, and two-level sigmoid functions describing the zero-plane-displacement parameter τ and the regression noise standard deviation σ. This means that the following regression was considered with the previously described informative prior:

$$R_i = \left[1 - \tau_1 - (\tau_2 - \tau_1)\frac{e^{\left(\frac{T_j - T_\tau}{s_\tau}\right)}}{1 + e^{\left(\frac{T_j - T_\tau}{s_\tau}\right)}}\right] e^{-\left(\frac{V_i}{\theta}\right)^\beta} + \tau_1 + (\tau_2 - \tau_1)\frac{e^{\left(\frac{T_j - T_\tau}{s_\tau}\right)}}{1 + e^{\left(\frac{T_j - T_\tau}{s_\tau}\right)}} + \sigma(T_i)\varepsilon_i \quad (9)$$

where the associated standard deviation of the regression noise is given by:

$$\sigma(T_i) = \sigma_1 + (\sigma_2 - \sigma_1)\frac{e^{(T_i - T_\sigma)/s_\sigma}}{1 + e^{(T_i - T_\sigma)/s_\sigma}} \quad (10)$$

Equation (10), describing the noise, shows some signs of unequal noise variance when plotted against true precipitation.

The posterior results in the form of histograms of MCMC samples are shown in Fig. 7. Parameter estimates, in the form of the means of the marginal posterior distributions, along with associated 95 % credibility intervals are displayed in Table 1a and b. The posterior distributions are much narrower than the corresponding prior distributions, suggesting that the choice of prior had little influence on the parameter estimates. The posteriors show little sign of complexities such as multimodality and heavy tails. Further, the parameters, which are invariant of the height of the wind speed measurements ($\tau_1, \tau_2, T_\tau, s_\tau$), do not show any practical difference, see Table 1. Performing the same analysis with an unfiltered data set, however, showed a noticeable difference in these parameters, implying that the filtering of the data was a justifiable procedure. The posterior results of that analysis are listed in Table 2.

As expected, both parameters (θ) and (β) seem to increase as a function of wind speed measurement height. Finally, the analysis with 10 m wind speed data yielded

HESSD
11, 10043–10084, 2014

a higher BML than the analysis using wind speed measured at gauge height. This fact indicates that the Bayesian analysis favours the 10 m wind speed data set for the chosen model form. A possible reason might be the better data quality of the 10 m wind speed measurements than of the gauge-height measurements despite the applied filtering. In any case, the adjustment functions (ignoring the noise term) are explicitly given by:

$$p_T = p_M \left\{ \left[0.82 - \frac{0.81 e^{\left(\frac{T-0.69}{1.15}\right)}}{1 + e^{\left(\frac{T-0.69}{1.15}\right)}} \right] e^{-\left(\frac{V}{3.41}\right)^{1.58}} + \frac{0.81 e^{\left(\frac{T-0.69}{1.15}\right)}}{1 + e^{\left(\frac{T-0.69}{1.15}\right)}} + 0.18 \right\}^{-1} \quad (11)$$

for wind speed measured at gauge height and:

$$p_T = p_M \left\{ \left[0.82 - \frac{0.81 e^{\left(\frac{T-0.66}{1.07}\right)}}{1 + e^{\left(\frac{T-0.66}{1.07}\right)}} \right] e^{-\left(\frac{V}{4.24}\right)^{1.81}} + \frac{0.81 e^{\left(\frac{T-0.66}{1.07}\right)}}{1 + e^{\left(\frac{T-0.69}{1.07}\right)}} + 0.18 \right\}^{-1} \quad (12)$$

for wind speed measured at 10 m.

The results for both adjustment equations are shown in Fig. 8. The upper part shows the results for wind at gauge height, Eq. (11), and the lower part the results for wind at 10 m, Eq. (12).

4.1 Analysis of residuals

How well the derived function and associated covariates describes the actual catch ratio can be evaluated with a closer look on the residuals. Standardised residuals, which are the original residuals normalised to have zero expectation and unit variances, are plotted in Fig. 9.

No signs of model misspecification can be seen for the covariates wind speed and temperature. Plotting the residuals against the true precipitation, measured in the DFIR, yields a trumpet shape, which may indicate that the noise variance is dependent of the amount of true precipitation. The panel, showing the theoretical quantils of a normal

HESSD
11, 10043–10084, 2014

distribution vs. the actual sample quantils, reveals that the residuals have a heavier tail than a normal distribution, which also indicates a non-sufficient description of the noise or uncertainty of the adjusted values.

5 Discussion and outlook

Three winters with precipitation data were collected and analysed during the study. Precipitation events were identified and afterwards filtered in order to pick only those events which were not disturbed by not-controllable parameters, as for example affected wind measurements. The classification of the dataset after key parameters which possibly influence precipitation loss gave a good idea of the shape of possible adjustment functions. Bayesian statistics were then used to more objectively choose the model describing the data set best. Only wind speed and air temperature are input variables for the derived adjustment. It calculates the catchment efficiency of a Geonor with Alter windshield compared to Geonor inside a double fence construction.

It was refrained from transferring the results further to meet values a bush-gauge would have measured. A bush-gauge, a precipitation gauge surrounded by equally distributed bushes of similar height, is generally been seen as the best method to measure true precipitation (Goodison et al., 1998). However, the existing transfer functions between precipitation data from a DFIR/DFIR to a bush gauge (Yang, 2014) are only valid for wind speeds below 9 m s^{-1} as no data for higher wind speeds exists.

5.1 Representativeness

The available dataset with events from 13 effective measurement months contained a huge variety of wind speeds. Wind speeds as high as 15–20 m s^{-1} as event average frequently occurred. That allowed for the first time to derive an adjustment function with a data-tested validity beyond 7 m s^{-1} and proved the stabilisation of the wind-induced precipitation loss for higher wind speeds. It also let expect that extrapolation for even

HESSD
11, 10043–10084, 2014

higher wind speeds is possible, in contrary to earlier equations where an extrapolation beyond the area of validity was accompanied by unrealistic changes in the catchment efficiency.

In this study, wind speed was measured with sensors mounted at 10 m height (WMO standard) as well as at gauge height. Both datasets were used and two different versions of the adjustment function were determined, to be used with 10 m or gauge height wind, respectively. All gauges at Haukeliseter are mounted at 4.5 m and the adjustment of the measured precipitation was invariant to the used wind data and adjustment function version. That might be different for gauges with another installation height. A lower gauge height, for example, would result in a larger difference between 10 m and gauge height winds. The use of wind data at gauge height is therefore recommended wherever possible.

The developed adjustment function is solely based on winter data. Nevertheless, quite mild events are also part of the analysis (up to ca. 6–7 °C average temperature), thus covering all three major precipitation types: snow, mixed precipitation, and rain. The results for the analysed warmer rain events are very clear and consistent. Summer precipitation, however, can be characterized by a larger variety of rain types, covering very light long lasting drizzle to heavy rain or hail showers, thus going along with huge variation of intensity and amount which was not covered by the present study. An application for temperature $> 3\,^{\circ}C$ is therefore not recommend, until studies evaluating explicitly summer precipitation are available.

Non-systematic scatter could be reduced significantly by means of relevant filters before the Bayesian statistic was applied. The necessity of this method could be confirmed by a comparison with an adjustment function based on the unfiltered data set which showed to be far less representative for the entire data set.

The scatter, however, was not extinguished completely. A natural variety of the catch efficiency between individual events remained, especially distinct for mixed precipitation events. Consequently, the resulting adjustment function is not correcting the precipitation amount perfectly, i.e. adjusting individual events can result in over or

HESSD
11, 10043–10084, 2014

underestimation of the true amounts. An application of the adjustment functions over a longer period, however, should balance out these errors.

Precipitation data sets from operational stations can contain accumulation records not related to precipitation. Wind measurements from wind sensors which are not adequately mounted, might lack the necessary quality for a successful use of the adjustment function. This study showed the importance of an extensive quality control of the observations before the application of the adjustment function.

In Norway, as well as in other countries, the most usual reporting interval at automated weather stations is one hour and the adjustment functions are optimized for that time interval. Historically, larger time intervals (12 and 24 h) were widely-used. The adjustment function was successfully applied for these longer time intervals for the available data from Haukeliseter in preliminary tests. Precipitation events during longer time intervals, however, happen not necessarily at times which are representative for the average wind speed or temperatures and larger uncertainties has to be calculated for when correcting the precipitation loss.

The question if the results are transferable to other stations can only be answered from a synoptic perspective. The thirteen analysed winter months covered a broad variety of wind speeds and temperature during precipitation events and thus providing data covering the climate variations which can be expected in the Norwegian mountains.

However, the influence of other parameters, as humidity or pressure, has not been studied. How far the presented adjustment study is valid for sites in other climates and at other altitudes is therefore not known. The cooperation within WMO SPICE, with 20 sites at very different climates, will help to answer this question.

5.2 Comparison with former model

The new adjustment function is based on sufficient data covering low and high windspeeds, thus allowing an extension of the validity beyond 7 m s^{-1} up to 15–20 m s^{-1}. Furthermore, it is suitable for all precipitation types, hence avoiding discontinuities resulting from the use of different equations for each phase. Comparisons with the old

HESSD
11, 10043–10084, 2014

equation set by Førland et al. (1996) do not show significant differences for the adjustment of snow events, given that the wind speed is below $7\,m\,s^{-1}$ and the temperature not very low. It can easily be seen that the old equation quickly approaches zero as the wind speed grows beyond $7\,m\,s^{-1}$, yielding unrealistic large amounts of precipitation. A truncation, where wind speeds above $7\,m\,s^{-1}$ are set to $7\,m\,s^{-1}$, is therefore commonly applied in Norway. Even then, the framework by Førland et al. (1996) differs quite largely from the one presented in this paper. Figure 10 shows that for temperatures close to 0 °C, the truncated version of the old equation adjusts up to 50 % more precipitation than the new one for wind speeds above $7\,m\,s^{-1}$. This over-correction is still present for wind speeds below $7\,m\,s^{-1}$, then decreases with further decreasing wind speeds. A comparison for temperatures above zero was not performed since this involves a third determinant, intensity, in the old correction method.

5.3 Regression noise and uncertainty analysis

As seen in the residual analysis, the regression noise is not optimally described with Equation (10). There are quite clear indications of heteroscadasticity in the residuals for increasing true precipitation. Heteroscedasticity is not expected to create any bias, but uncertainty analysis could be inaccurate. Heavy tailed characteristics were also noted. This suggests that the residual distribution belongs to another family than the normal distribution. Though symmetry about zero still seems to be the case and systematics bias in estimates is avoided, uncertainty analysis becomes imprecise and adding to the problems caused by heteroscadasticity. Also, and perhaps more important, is how the regression result is used in this study. It is applied in an inverted form to derive the true precipitation from the ratio. The statistical properties of this quantity, which in the Bayesian formulation is a distribution, are not clear. Adding the fact that the noise is subject to misspecification, makes uncertainty analysis about the true precipitation estimate substantially unreliable at this stage.

These two aforementioned statistical issues, the distribution of the inversion and specification of the regression noise, were beyond the scope of this study, which major

HESSD
11, 10043–10084, 2014

objective was to develop an adjustment function for measured precipitation. Further investigations with alternative regression models able to deliver a more trustable framework for the uncertainty analysis are currently in progress.

6 Conclusions

Extensive measurements over three winter seasons have given new insight in under-catch of solid precipitation due to wind. Also, a better understanding of the sources of error for measuring precipitation is gained. The measurements performed at Haukeliseter are unique, given the wide range of wind speeds and snow amounts which were observed.

Clear differences are seen for precipitation classified as dry snow, mixed precipitation and rain when analysing wind induced under-catch. The under-catch has a pronounced relation to temperature and a non-linear relation to wind speed. For solid precipitation at −2 °C or below, only 80 % of the assumed true precipitation is caught at wind speeds of 2 m s^{-1}, and only 40 % at 5 m s^{-1}. The slope of the catch ratio then subsides remarkably and stabilizes at 20 % at 7–8 m s^{-1}. This base line level is confirmed with data up to 15–20 m s^{-1} and will most likely not change for even higher wind speeds.

This is the first time that under-catch of snow at these very high wind speeds in mountainous areas could be documented with observed data. Previous studies assumed a stabilization of the catch ratio for wind speeds above 7 m s^{-1}, but have up to now not been able to show this explicitly due to poor data coverage.

Because of the variation in the aerodynamical properties for wet snow and mixed precipitation, the results are less unambiguous at temperatures between −2 to 2 °C.

Results for the precipitation events at even higher temperatures, above 2–3 °C, and thus rain, show a quite small under-catch, especially for wind speeds below 11 m s^{-1}.

Based on this broadly based data set, a new adjustment function for winter precipitation measured by an automatic precipitation gauge (Geonor) equipped with a single Alter wind shield, was established. With the means of Bayesian statistics the model

HESSD
11, 10043–10084, 2014

which describes the observations best, was selected. The result is one continuous equation which describes the wind induced under-catch for snow, mixed precipitation and rain events for wind speeds up to at least 20 m s^{-1} and temperatures up to 3 °C. Input parameters are wind speed and air temperature, thus allowing for easy application at operational weather stations only equipped with basic sensors. Originally, the adjustment function is developed for hourly precipitation measurements. However, first tests of the function show promising results for 12 and 24 h as well.

Residual analysis of the adjustment function could not reveal any signs of misspecifications of the chosen model. The accompanying noise-model, however, seems to not adequately describe the uncertainty of the adjustment and requires further investigation. Preliminary studies, however, let expect that an improvement of the noise-model will be possible without changes in the adjustment function itself.

Beside its original purpose, the site is also a host-site for WMO-SPICE. Furthermore, the Norwegian Meteorological Institute will operate the DFIR at Haukeliseter as a long-term reference to monitor the changes in precipitation amount in Norway. The station is also part of an increasing network for supporting improved avalanche forecasting in Norway.

Acknowledgements. The presented study was funded by Energi Norge (project no. Sy-PD-1.4_09) with contributions from Statkraft, Norsk Hydro ASA, BKK, Agder Energi Prod., Lyse Produksjon AS, E-CO Energi AS, Nord-Trøndelag Elektrisitetsverk, Glommens og Laagens Brukseierforening and Trønder Energi. Large parts of the data collection and transfer, maintenance work and analysis was provided by the Norwegian Meteorological Institute and Statkraft free of charge.

Parts of the data presented in this work will also be used for SPICE, conducted on behalf of the World Meteorological Organization (WMO) Commission for Instruments and Methods of Observation (CIMO). The analysis and views described herein are those of the authors at this time, and do not necessarily represent the official outcome of WMO SPICE. Mention of commercial companies or products is solely for the purposes of information and assessment within the scope of the present work, and does not constitute an endorsement by the authors or WMO.

HESSD
11, 10043–10084, 2014

We thank Erik Ruud (formerly Statkraft) who played a major role developing the framework of a full-size and fundable project, starting from just a few ideas on how to improve the automated precipitation measurements in Norway. Our thanks go to Tom Andersen (Statkraft) who inspired many of the contributors to support the project through Energi Norge.

We are grateful to Eirik Førland (MET Norway) for sharing his in-depth knowledge of the existing adjustment functions and long experience on analyzing precipitation data.

We appreciated the engaged work of Sverre Nylend (Statkraft) and Ole-Jørgen Østby (MET Norway) who spent many hours with installation and maintenance work at the site. Åse Moen Vidal, Ola Bondlid, Terje Reite, Rune Ringberg and Arne Sund (all MET Norway) are acknowledged for realizing the data collection and storage and general IT support.

References

Barnett, T. P., Adam, J. C., and Lettenmaier, D. P.: Potential impacts of a warming climate on water availability in snow-dominated regions, Nature, 438, 303–309, 2005.

Bindoff, N. L., Stott, P. A., AchutaRao, K. M., Allen, M. R., Gillett, N., Gutzler, D., Hansingo, K., Hegerl, G., Hu, Y., Jain, S., Mokhov, I. I., Overland, J., Perlwitz, J., Sebbari, R., and Zhang, X.: Detection and attribution of climate change: from global to regional, in: Climate Change 2013: The Physical Science Basis. Contribution of Working Group I to the Fifth Assessment Report of the Intergovernmental Panel on Climate Change, edited by: Stocker, T. F., Qin, D., Plattner, G.-K., Tignor, M., Allen, S. K., Boschung, J., Nauels, A., Xia, Y., Bex, V., and Midgley, P. M., Cambridge University Press, Cambridge, UK and New York, NY, USA, 867–952, 2013.

Brown, M. J. and Peck, E. L.: Reliability of precipitation measurements as related to exposure, J. Appl. Meteorol., 1, 203–207, 1962.

Chib, S. and Greenberg, E.: Understanding the Metropolis–Hastings Algorithm, Am. Stat., 49, 327–335, 2001.

Førland, E. J., Allerup, P., Dahlström, B., Elomaa, E., Jónsson, T., Madsen, H., Perälä, J., Rissanen, P., Vedin, H., Vejen, F.: Manual for operational correction of Nordic precipitation data. DNMI report Nr. 24/96, Norwegian Meteorological Institute, Oslo, Norway, 1996.

Førland, E. J. and Hanssen-Bauer, I.: Increased precipitation in the Norwegian Arctic: true or false?, Clim. Change, 46, 485–509, 2000.

HESSD

11, 10043–10084, 2014

Gelman, A., Carlin, J. B., Stern, H. S., Dunson, D. B., Vehtari, A., and Rubin, D. B.: Bayesian Data Analysis, 3rd ed., Chapman & Hall, United States, 2013.
Goodison, B. E., Louie, P. Y. T., and Yang, D.: WMO solid precipitation measurement intercomparison: final report, Instruments and Observing Methods Rep. 67, WMO/TD-No. 872, World Meteorological Organization, Geneva, Switzerland, 1998.
Hanssen-Bauer, I., Førland, E. J., and Nordli, P.Ø.: Measured and true precipitation at Svalbard, DNMI report Nr. 31/96, Norwegian Meteorological Institute, Oslo Norway, 1996.
Nešpor, V. and Sevruk, B.: Estimation of wind-induced error of rainfall gauge measurements using a numerical simulation, J. Atmos. Ocean. Tech., 16, 450–464, 1999.
Nitu, R. and Wong, K.: CIMO survey on national summaries of methods and instruments for solid precipitation measurement at automatic weather stations, Instruments and Observing Methods Report No. 102, WMO/TD-No. 1544, World Meteorological Organization, Geneva, 2010.
Rasmussen, R., Baker, B., Kochendorfer, J., Meyers, T., Landolt, S., Fischer, A. P., Black, J.,Thériault, J., Kucera, P., Gochis, D., Smith, C., Nitu, R., Hall, M., Cristanelli, S., and Gutmann, E.: How well are we measuring snow?, B. Am. Meteorol. Soc., 93, 811–829, doi:10.1175/BAMS-D-11-00052.1, 2012.
Reitan, T. and Petersen-Øverleir, A.: Bayesian power-law regression with a location parameter, with applications for construction of discharge rating curves, Stoch. Environ. Res. Risk. Assess., 22, 351–365, doi:10.1007/s00477-007-0119-0, 2008.
Reitan, T. and Petersen-Øverleir, A.: Bayesian methods for estimating multi-segmented discharge rating curves, Stoch. Env. Res. Risk A, 23, 627–642, 2009.
Seneviratne, S. I., Nicholls, N., Easterling, D., Goodess, C. M., Kanae, S., Kossin, J., Luo, Y., Marengo, J., McInnes, K., Rahimi, M., Reichstein, M., Sorteberg, A., Vera, C., and Zhang, X.: Changes in climate extremes and their impacts on the natural physical environment, in: Managing the Risks of Extreme Events and Disasters to Advance Climate Change Adaptation. A Special Report of Working Groups I and II of the Intergovernmental Panel of Climate Change (IPCC). Cambridge University Press, Cambridge, UK, and New York, NY, USA, 109–230, 2012.
Sevruk, B.: Methods of correction for systematic error in point precipitation measurement for operational use, Operational Hydrology Rep. 21, WMO Rep. 589, 91 pp., Geneva, Switzerland, 1982.

HESSD
11, 10043–10084, 2014

Smith, C. D. and Yang, D.: An assessment of the GEONOR T-200B inside a large octagonal double fence wind shield as an automated reference for the gauge measurement of solid precipitation, in: Proceedings of the 90th AMS Annual Meeting, American Met. Soc., Atlanta, GA, 2010.

Thériault, J. M., Rasmussen, R., Ikeda, K., and Landolt, S.: Dependence of Snow Gauge Collection Efficiency on Snowflake Characteristics, J. Appl. Meteor. Climatol., 51, 745–762, 2012.

WMO/CIMO, International Organizing Committee for the WMO Solid Precipitation Intercomparison Experiment: Final Report of the Second Session, Boulder, USA, WMO, Geneva, 74 pp., 2012.

Wolff, M., Brækkan, R., Isaksen, K., and Ruud, E.: A new testsite for wind correction of precipitation measurements at a mountain plateau in southern Norway, in: Proceedings of WMO Technical Conference on Meteorological and Environmental Instruments and Methods of Observation (TECO-2010). Instruments and Observing Methods Report No. 104, WMO/TD-No. 1546, World Meteorological Organization, Geneva, 2010.

Wolff, M., Isaksen, K., Brækkan, R., Alfnes, E., Petersen-Øverleir, A., and Ruud, E.: Measurements of wind-induced loss of solid precipitation: description of a Norwegian field study, Hydrology Res., 44, 35–43, doi:10.2166/nh.2012.166, 2013.

Yang, D., Kane, D., Zhang, Z., Legates, D., and Goodison, B.: Bias corrections of long-term (1973–2004) daily precipitation data over the northern regions, Geophys. Res. Lett., 32, L19501, doi:10.1029/2005GL024057, 2005.

Yang, D.: Double Fence Intercomparison Reference (DFIR) vs. Bush Gauge for "true" snowfall measurement, J. Hydrol., 509, doi:10.1016/j.jhydrol.2013.08.052, 2014.

HESSD
11, 10043–10084, 2014

Table 1. Estimated parameters for the adjustment function, Eq. (9) and the standard deviation of the regression noise, Eq. (10), for two data sets. Each parameter is represented with three values: upper and lower 95 % confidence interval and the best estimate in the middle. The parameters for Eq. (9) are shown in (a), whereas the parameters for Eq. (10) are shown in (b).

(a)

	θ	β	τ_1	τ_2	T_τ	s_τ
Gauge-height-wind data set	(2.89, **3.41**, 4.18)	(1.19, **1.58**, 2.20)	(0.10, **0.18**, 0.27)	(0.96, **0.99**, 1.00)	(0.29, **0.69**, 1.09)	(0.89, **1.15**, 1.50)
10 m wind data set	(4.02, **4.24**, 4.48)	(1.62, **1.81**, 2.03)	(0.14, **0.18**, 0.22)	(0.98, **0.99**, 1.00)	(0.48, **0.66**, 0.84)	(0.93, **1.07**, 1.21)

(b)

	σ_1	σ_2	T_σ	s_σ
Gauge-height-wind data set	(0.21, **0.23**, 0.25)	(0.10, **0.13**, 0.16)	(1.17, **2.03**, 2.74)	(0.02, **0.40**, 1.04)
10 m wind data set	(0.17, **0.18**,0.19)	(0.09, **0.11**, 0.12)	(2.16, **2.35**, 2.83)	(0.00, **0.12**, 0.42)

HESSD
11, 10043–10084, 2014

Table 2. Estimated parameters for the adjustment function, Eq. (9), calculated with the unfiltered gauge-height-wind data set. Each parameter is represented with three values: upper and lower 95 % confidence interval and the best estimate in the middle.

	θ	β	τ_1	τ_2	T_τ	s_τ
Gauge-height-wind data set (unfiltered)	(3.57, **4.55**, 5.75)	(1.05, **1.43**, 1.87)	(0.26, **0.36**, 0.43)	(0.97, **0.99**, 1.00)	(0.94, **1.14**, 1.32)	(0.30, **0.44**, 1.60)

HESSD
11, 10043–10084, 2014

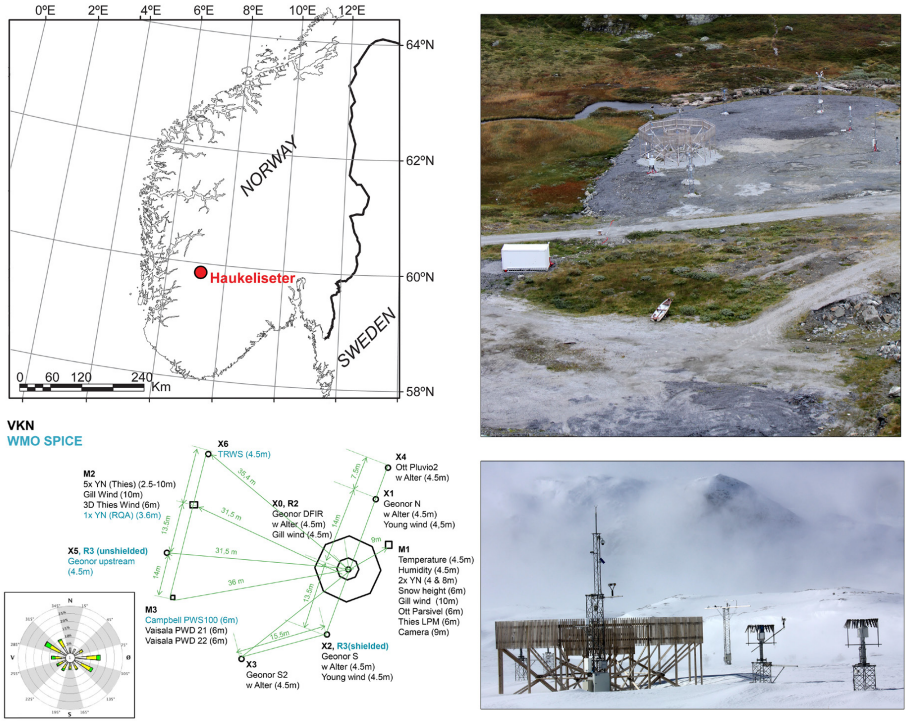

Figure 1. Localisation of the test site Haukeliseter in southern Norway (upper left). The lower left panel shows the layout of the site and a wind rose showing the statistical distribution of wind directions. The layout is orientated in the same way as the wind rose. The two photographs show the test site. The picture in the upper right was taken by Ole Jørgen Østby from aboard a helicopter. The picture in the lower right was taken by Roy Rasmussen.

HESSD
11, 10043–10084, 2014

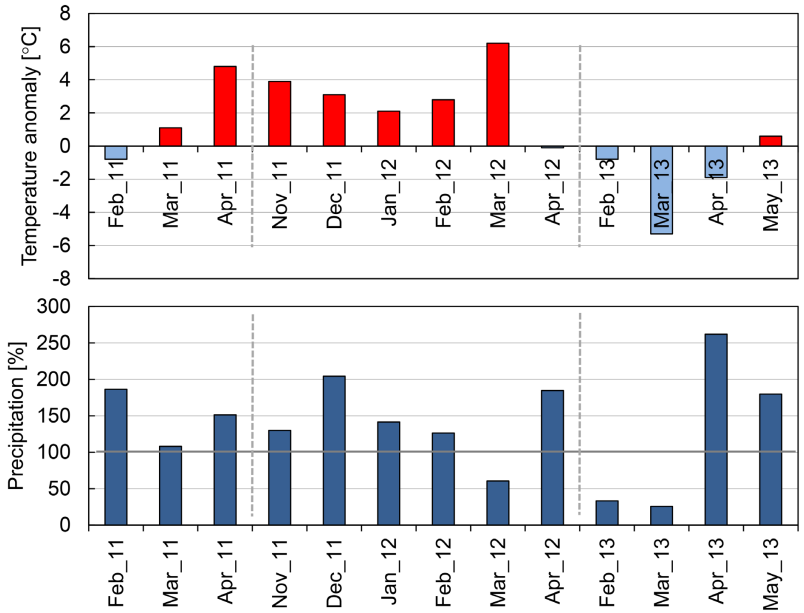

Figure 2. Temperature (top) and precipitation (bottom) anomaly in respect to normal period (1961–1990) at Vågsli, the closest official weather station to Haukeliseter.

HESSD
11, 10043–10084, 2014

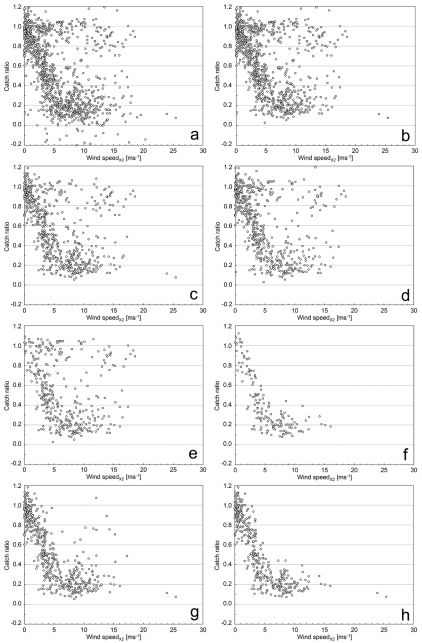

Figure 3. Catch ratio between Geonor South (X2) and DF-Geonor vs. wind speed (measured at gauge height). Different filters are applied on all one-hour precipitation events from three winter seasons (2011–2013). **(a)** shows all precipitation events without filter. **(b)** shows events where the accumulation measured by Geonor South (X2) was larger than 0.1 mm within the last hour. In **(c)**, an additional filter cut all events with an average wind direction between 355° and 55°, corresponding to the sector where a shadowing effect of the DFIR construction can be expected. **(d)** has an additional filter cutting all events where temperature standard deviation is exceeding 0.2 °C. **(e)** shows only event with additional low wind speed variations. The threshold was set to a maximum of 0.2 for the ratio between standard deviation and mean wind speed. On the data in **(f)** are the same filters applied as for data in **(e)**, only events with mean temperature below −2 °C are shown. (**g** and **h**) show data with the same filter applied as in **(c)**, for temperatures lower than 0 °C **(g)** and lower than −2 °C.

HESSD
11, 10043–10084, 2014

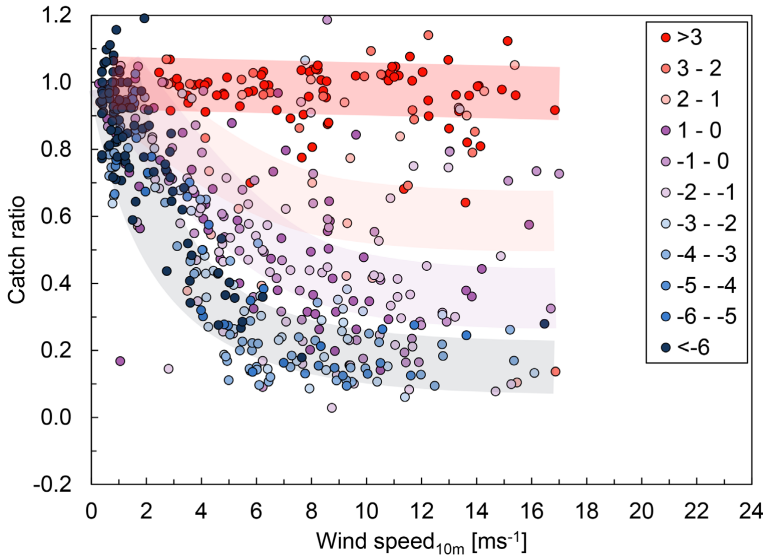

Figure 4. Catch efficiency of the south Geonor (X2) compared to DFIR for different wind speeds (10 m height), classified for temperature (color coded, see legend). Data are from 2011–2012. Data are filtered: a significant (> 0.1 mm) accumulation in the south Geonor was required; events with possible affected wind directions were neglected. The colored areas visualize the continuous temperature dependent change in the shape of the catch ratio curve.

HESSD
11, 10043–10084, 2014

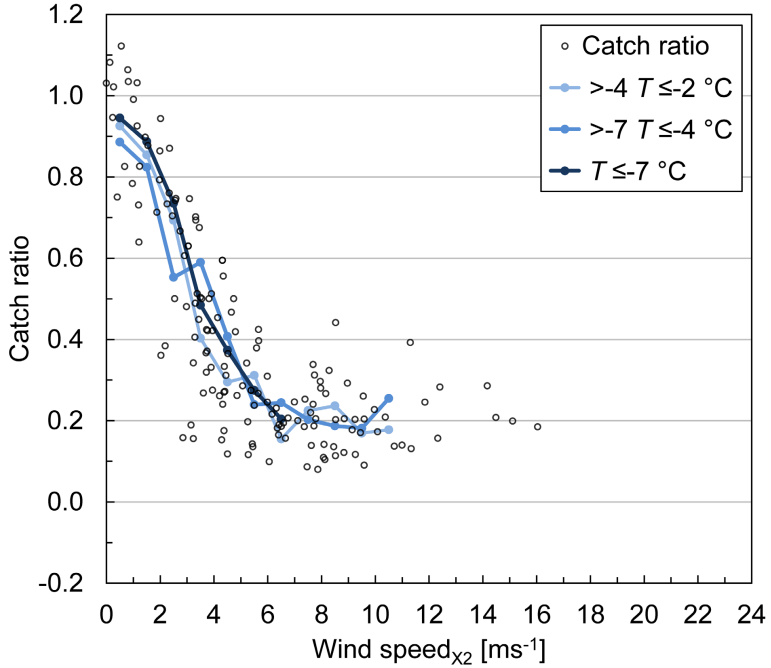

Figure 5. Catch ratio between the south Geonor (X2) and the DFIR-Geonor vs. windspeed. Only temperature classes where precipitation is expected as snow are shown. The overlaid curves show data collected into 1 m s^{-1} wind speed classes. Data from 2011–2013 are shown and filtered according to description of panel c in Fig. 3

HESSD
11, 10043–10084, 2014

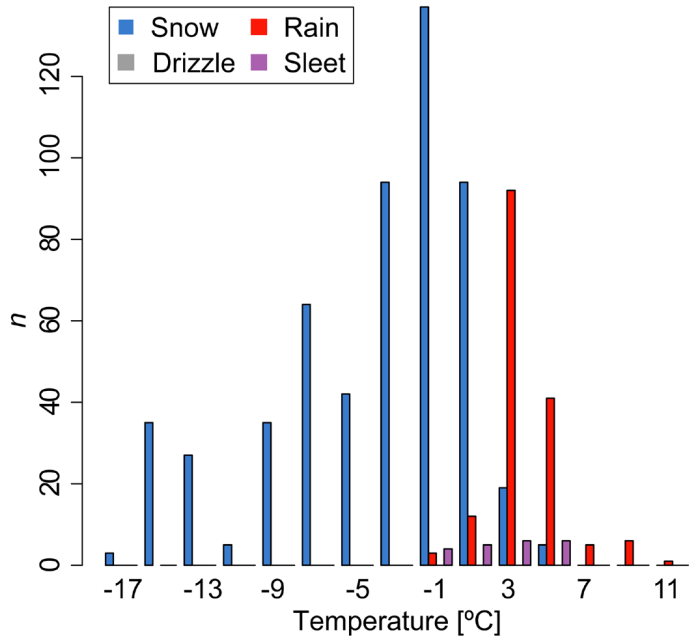

Figure 6. Number of events with different precipitation types and temperatures. Precipitation type is measured by a forward scatter type instrument (Vaisala PWD 21). Event data from 2011–2012 are shown.

HESSD
11, 10043–10084, 2014

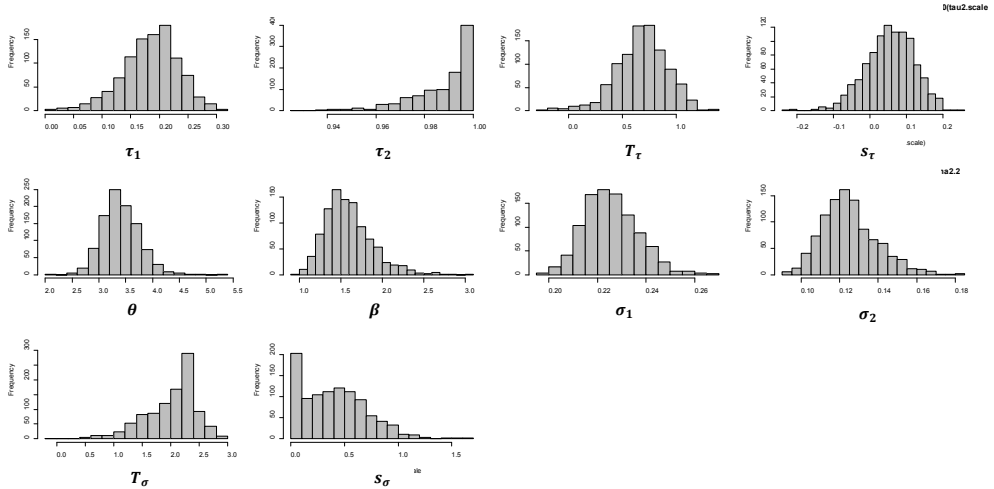

Figure 7. Plots showing the posterior distributions for the parameters in the analysis of the gauge-height wind data set.

HESSD
11, 10043–10084, 2014

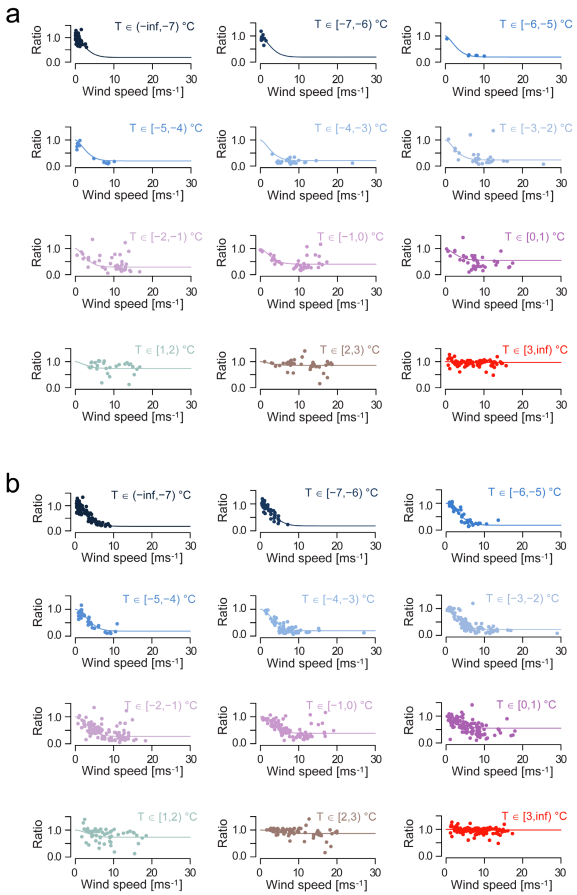

Figure 8. Adjustment function for wind in gauge height **(a)** and wind in 10 m **(b)** for various temperature classes. Adjustment function is calculated with the mean temperature of the individual classes.

HESSD
11, 10043–10084, 2014

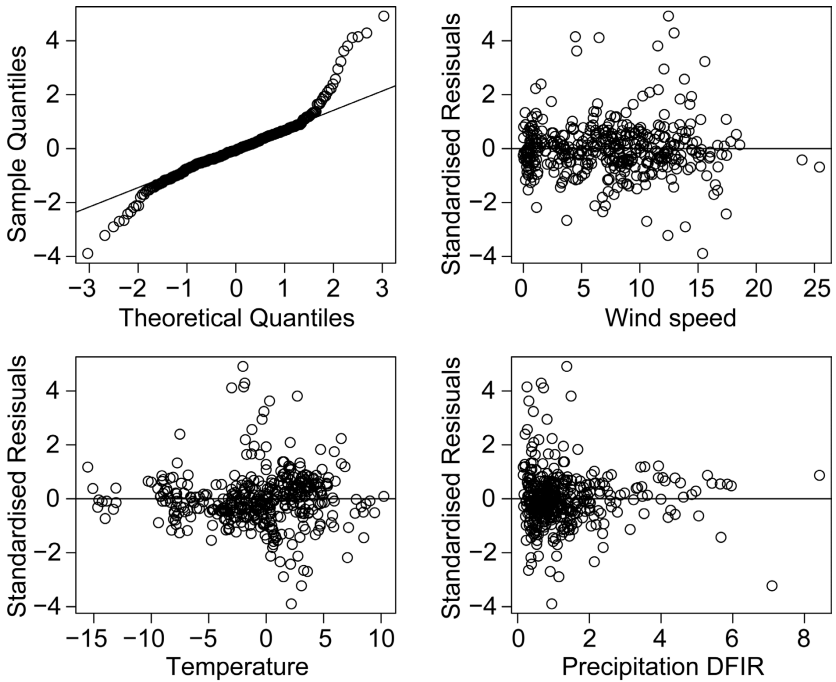

Figure 9. Standardised residuals, which are the raw residuals divided by their estimated standard deviation (bottom and top right) vs. wind speed (upper right), temperature (lower left) and precipitation amount (lower right). In the upper left panel the theoretical percentiles from the standard normal distribution are plotted vs. the empirical percentiles from the standardised residual distribution.

HESSD
11, 10043–10084, 2014

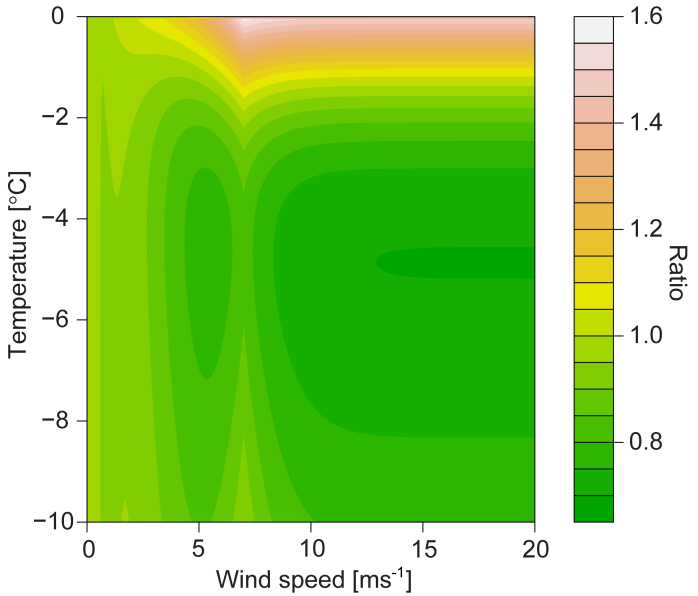

Figure 10. Contour plot showing the ratio between the former and commonly applied correction factor by Førland et al. (1996) and the correction factor presented in this paper. The correction factor is the factor which needs to be applied to the measured precipitation to obtain the true precipitation. Contours higher than one indicate that the method by Førland et al. gives more precipitation than the new adjustment equation. Note that the analysis by Førland et al. (1996) sets wind speeds above 7 m s^{-1} to 7 m s^{-1}.

HESSD
11, 10043–10084, 2014